Proceedings of the International Congress on Advances in Applied Physics and Materials Science, Antalya 2011

Growth and Characterization of Indium-Doped Zinc Oxide Thin Films Prepared by Sol–Gel Method

M.S. Kim[a], K.G. Yim[a], S. Kim[b], G. Nam[b], D.-Y. Lee[c], Jin Soo Kim[d], Jong Su Kim[e] and J.-Y. Leem[a,b,*]

[a]Department of Nano Systems Engineering, Center for Nano Manufacturing, Inje University Gimhae, Gyungnam 621-749, Republic of Korea

[b]School of Nano Engineering, Inje University, Gimhae, Gyungnam 621-749, Republic of Korea

[c]Epi R&D team, Samsung LED Co. Ltd., Suwon, Gyeonggi-do 443-373, Republic of Korea

[d]Research Center of Advanced Materials Development (RCAMD), Division of Advanced Materials Engineering Chonbuk National University, Jeonju, Chonbuk 561-756, Republic of Korea

[e]Department of Physics, Yeungnam University, Gyeongsan, Gyeongsangbuk-do 712-749, Republic of Korea

Indium-doped ZnO thin films were deposited by sol–gel spin-coating method with various In content. The effects of In content on the structural and optical properties of the indium-doped ZnO thin films were investigated by scanning electron microscopy, X-ray diffraction, and UV-visible spectroscopy. The particle-like surface morphology and the crystallinity of the indium-doped ZnO thin films were affected by change in the In content, especially at the In content of 3 at.%. The values of direct band gap were decreased with increase in the In content. The width of localized states in the optical band gap of the indium-doped ZnO thin films were changed with In content and the Urbach energy (E_U) was changed inversely with optical band gap of the indium-doped ZnO thin films.

PACS: 81.05.Dz, 81.20.Fw, 78.66.Hf

1. Introduction

Zinc oxide (ZnO) is a direct wide band gap semiconductor material (E_g = 3.37 eV at room temperature). It has a large excitation binding energy of 60 meV, which makes the exciton hard to be thermally ionized. In addition, ZnO is one of the II–VI compound semiconductors and is composed of hexagonal wurtzite crystal structure. As a matter of fact, ZnO has a variety of potential applications such as gas sensors [1], surface acoustic devices [2], transparent electrodes [3], and solar cells [4]. Various deposition techniques like sputtering [5], pulsed laser deposition (PLD) [6], chemical vapor deposition (CVD) [7], molecular beam epitaxy (MBE) [8], hydrothermal reaction [9], and sol–gel [10] have been widely employed in the deposition of ZnO thin films. Among them, the sol–gel method has some merits, such as the easy control of chemical components, and fabrication of thin films at a low cost to investigate structure and optical properties of ZnO thin films.

ZnO can be doped with a wide variety of ions to meet the demands of several application fields. Among the various dopants for *n*-type ZnO thin films, Al, Ga, and In have been determined to be the most suitable materials. It is well known that the physical characteristics of the ZnO thin films depend on the doping, and then a study of the doping effect on the physical characteristics is always interesting. However, there are a few reports on the In-doped ZnO thin films deposited by sol–gel method [11]. Therefore, in this paper, the effects of In content on structural and optical properties of In-doped ZnO thin films prepared by sol–gel method were studied.

2. Experimental details

The In-doped ZnO (IZO) thin films were deposited on quartz substrates by sol–gel spin-coating method. The precursor solution was prepared by dissolving 0.5 M zinc acetate dihydrate [$Zn(CH_3COO)_2 \cdot 2H_2O$] in 0.5 M 2-methoxyethanol as a solvent, and monoethanolamine (MEA) was added to the stable sol solution. The molar ratio of zinc acetate dihydrate to 2-methoxyethanol was maintained at 1:1. The In content was controlled by the change in the atomic% ratio of indium chloride ($InCl_3$) to zinc acetate dihydrate from 0 to 5. The resultant sol solution was stirred at 60 °C for 2 h to yield a clear and homogeneous solution. The sol solution was preserved

* corresponding author

for 24 h before the deposition of the IZO thin films. The sol solution was spin-coated onto quartz substrate, rotated at 3000 rpm for 20 s. The IZO thin films were heated at 300 °C for 10 min to evaporate the solvent and remove the organic residuals (named as pre-heat treatment). The spin-coating and pre-heating processes were repeated 5 times. In order to crystallize, the IZO thin films were heated in a furnace under an air atmosphere at 500 °C for 1 h (named as post-heat treatment). The effects of In content on the structural and optical properties of the IZO thin films were investigated by scanning electron microscopy (SEM), X-ray diffraction (XRD), and UV-visible spectroscopy.

3. Results and discussion

Figure 1 shows SEM images of the IZO thin films with different In content; (a) 0, (b) 1, (c) 2, (d) 3, (e) 4, and (f) 5 at.%. The IZO thin films exhibited a rough surface with a particle-like structure. The particle-like and pore structure was particularly apparent on the sol–gel synthesized ZnO thin films. By increase in the In content, the particle size was increased and the pores become larger. The IZO thin films consisted of two layers (bottom and upper layer). The bottom layer could be obviously observed as the particles of upper layer were merged by increase in the In content. The double layer is because of the ZnO thin films not being a high thermal resistance material, its thermal peeling behavior has still not been examined, especially under the sol–gel method [12].

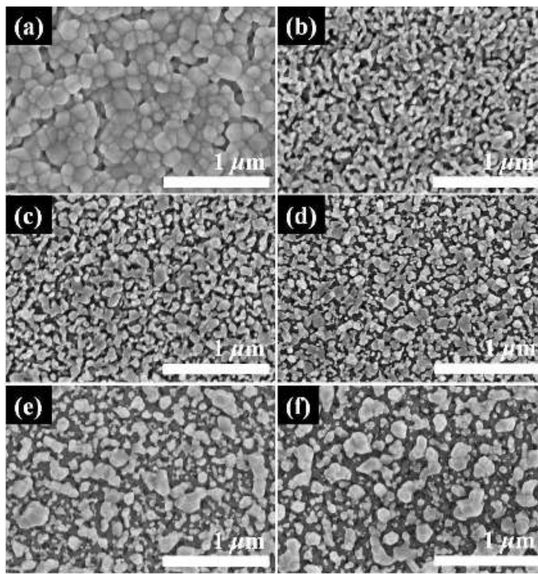

Fig. 1. SEM images of the IZO thin films with different In content: (a) 0, (b) 1, (c) 2, (d) 3, (e) 4, and (f) 5 at.%.

Figure 2 shows XRD pattern of the IZO thin films with different In content: (a) 0, (b) 1, (c) 2, (d) 3, (e) 4, and (f) 5 at.%. From undoped ZnO thin films, seven ZnO diffraction peaks at 31°, 34°, 36°, 47°, 56°, 63°, and 68° were observed, corresponding to ZnO (100), ZnO (002), ZnO (010), ZnO (102), ZnO (110), ZnO (103), and ZnO (200), respectively. It is well known that ZnO is usually grown with *c*-axis preferred orientation under typical growth conditions due to the lowest surface energy of the (001) basal plane in ZnO, leading to a preferred growth in the [001] direction. With increase in the In content to 3%, the intensity of the ZnO (002) diffraction peak was increased while that of the other diffraction peak was decreased. This implies that the crystal quality is improved by In doping. However, by further increase in the In content, the intensity of the ZnO (002) diffraction peak was decreased as shown in Fig. 3A.

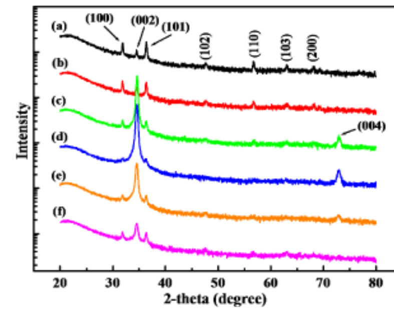

Fig. 2. XRD pattern of the IZO thin films with different In content: (a) 0, (b) 1, (c) 2, (d) 3, (e) 4, and (f) 5 at.%.

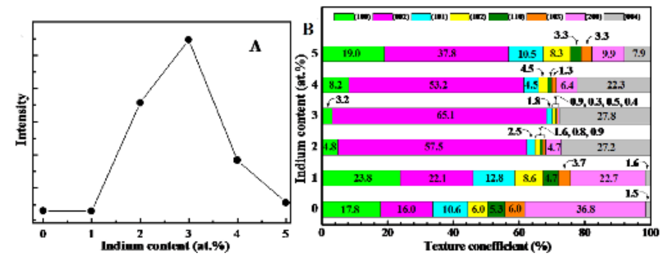

Fig. 3. The intensity of ZnO (002) diffraction peak and texture coefficient of the IZO thin films with various In content.

In order to describe the preferred orientation, the texture coefficient ($TC_{(hkl)}$) was calculated using the following equation [13]:

$$TC_{(hkl)} = (I_{(hkl)}/I_{0(hkl)}) \Big/ \left[1/N \sum_N I_{(hkl)}/I_{0(hkl)} \right], \tag{1}$$

where N is the number of diffraction peaks, $I_{(hkl)}$ and $I_{0(hkl)}$ are the integrated intensities corresponding to the (*hkl*) reflection of the IZO thin films containing the textured and randomly oriented crystallites. It is clear from the definition that the deviation of TC from unity implies the IZO thin films growth in preferred orientation along that diffraction plane. As shown in Fig. 3B, the value of the $TC_{(002)}$ and $TC_{(004)}$, which indicate the *c*-axis preferred orientation, was increased with increasing the In

content to 3%. However, the value of the $TC_{(002)}$ and the $TC_{(004)}$ was decreased by further increase in the In content. These results indicate that the crystal quality of the IZO thin films is improved by incorporation with adequate amounts of In. It might be because the crystalline of the IZO thin films became more perfect. The migration velocity of In is faster than Zn and O atoms in the ZnO due to the weaker In–O bond than Zn–O bond. The In atoms could have more chance to reach Zn lattice site earlier than O atoms during the pre- and post-heat treatment, and O antisites would be reduced, consequently the c-axis preferred orientation and the crystallinity of the IZO thin films was enhanced.

Figure 4 shows optical transmittance of the IZO thin films with different In content in the range from 0 to 5 at.%. The optical transmittance of the IZO thin films is determined by the thickness, surface roughness, and the absorption coefficient of the sample [14]:

$$T = \exp(-\alpha(\lambda)d), \tag{2}$$

where T is the transmittance, α is the absorption coefficient, and d is the thickness of the IZO thin films. The absorption edge of optical transmittance for the IZO thin films was affected by the change of In content. The fundamental absorption edge of the IZO thin films corresponds to electron transitions from valence band to conduction band and this edge can be used to calculate the optical band gap of the IZO thin films. In the direct transition, the absorption coefficient can be expressed by [15]:

$$\alpha = C\left(h\nu - E_g\right)^n / h\nu, \tag{3}$$

where C is a constant, $h\nu$ is the photon energy and E_g is the optical band gap. If the material has a indirect band gap, n is 2; if the material has a direct band gap, n is 1/2.

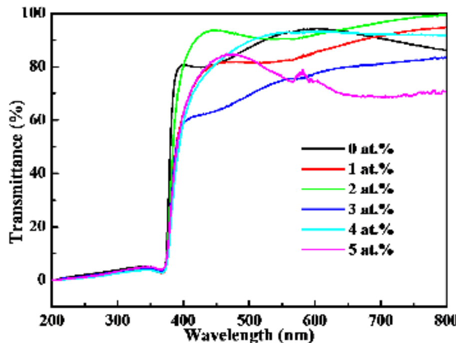

Fig. 4. Optical transmittance of the IZO thin films with various In content.

Figure 5 shows plots of $(\alpha h\nu)^2$ vs. photon energy. The E_g values of the IZO thin films were calculated from these plots. As seen from these plots, E_g values of the IZO thin films were decreased from 3.2906 to 3.2560 eV with increase in the In content. Bae et al. [16] reported the redshift of E_g by In doping in ZnO. The incorporation of In is accompanied by a systematic low-energy shift of the band gap extending down to the yellow spectral range. The narrowing band gap energy is possibly due to the existence of In impurities in Zn, which induce the formation of new recombination centers with lower energy state. The increase in the E_g should be also caused by the increasing carrier concentration with In incorporation.

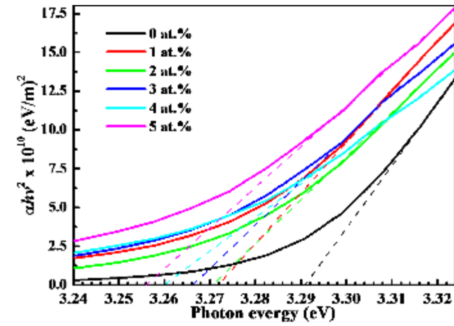

Fig. 5. The plots of $(\alpha h\nu)^2$ vs. photon energy of the IZO thin films with various In content.

The incorporation of impurity into the semiconductor often reveals the formation of band in the band gap. The absorption coefficient near fundamental absorption edge is exponentially dependent on the incident photon energy and obeys the empirical Urbach relation, where $\ln\alpha$ varies as a function of $h\nu$. The Urbach energy can be calculated by the following relation [17]:

$$\alpha = \alpha_0 \exp(h\nu/E_U), \tag{4}$$

where α_0 is a constant and E_U is the Urbach energy which refers the width of the exponential absorption edge.

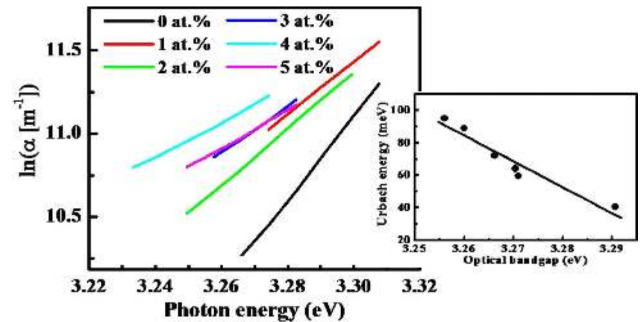

Fig. 6. The Urbach plots and the plots of the E_U vs. optical band gap of the IZO thin films.

Figure 6 shows (A) the variation of $\ln\alpha$ vs. photon energy and (B) E_U vs. optical band gap for the IZO thin films. The E_U values were calculated from the Urbach plots using following relation:

$$E_U = [\mathrm{d}(\ln\alpha)/\mathrm{d}(h\nu)]^{-1}. \tag{5}$$

The E_U value of the IZO thin films was gradually increased from 40.4 to 94.8 meV as the In content increased. The In content was responsible for the width of localized states in the optical band of the IZO thin films and it decreases the width of localized states in the optical band

gap. Thus, the E_U value was inversely changed with optical band gap of the IZO thin films as shown in Fig. 6B.

4. Conclusions

The IZO thin films were deposited by sol–gel spin-coating method with various In content. All IZO thin films show a particle-like structure and the surface morphology is affected by the In content. The crystal quality and *c*-axis preferred orientation of the IZO thin films are enhanced by In content, especially at the In content of 3 at.%. The values of direct band gap were decreased with increase in the In content. The width of localized states in the optical band gap of the IZO thin films were changed with In content and the E_U was changed inversely with optical band gap of the IZO thin films.

Acknowledgments

This research was supported by Basic Science Research Program through the National Research Foundation of Korea (NRF) funded by the Ministry of Education, Science and Technology (No. 2011-0003067).

References

[1] M. Suchea, S. Cheristoulakis, K. Moschovis, N. Katsarakis, G. Kiriakidis, *Thin Solid Films* **515**, 551 (2006).

[2] W. Water, S.-Y. Chu, Y.-D. Juang, S.-J. Wu, *Mater. Lett.* **57**, 998 (2002).

[3] F. Michelotti, A. Belardini, A. Rousseau, A. Ratsimihety, G. Schoer, J. Mueller, *J. Non-Cryst. Solids* **352**, 2339 (2006).

[4] J. Hupkes, B. Rech, O. Kluth, T. Repmann, B. Zwaygardt, J. Muller, R. Drese, M. Wuttig, *Sol. Energy Mater. Sol. Cells* **90**, 3054 (2006).

[5] Y. Zhang, G. Du, D. Liu, X. Wang, Y. Ma, J. Wang, J. Yin, X. Yang, X. Hou, S. Yang, *J. Cryst. Growth* **243**, 439 (2002).

[6] J.L. Zhao, X.M. Li, J.M. Bian, W.D. Yu, X.D. Gao, *J. Cryst. Growth* **276**, 507 (2005).

[7] Y. Zhang, G. Du, B. Zhang, Y. Cui, H. Zhu, Y. Chang, *Semicond. Sci. Technol.* **20**, 1132 (2005).

[8] M.Y. Cho, M.S. Kim, H.Y. Choi, S.M. Jeon, G.S. Kim, D.Y. Kim, K.G. Yim, D.-Y. Lee, J.S. Kim, J.S. Kim, J.I. Lee, J.-Y. Leem, *J. Korean Phys. Soc.* **56**, 1833 (2010).

[9] M.S. Kim, K.G. Yim, M.Y. Cho, D.-Y. Lee, J.S. Kim, J.S. Kim, J.-S. Son, J.-Y. Leem, *J. Korean Phys. Soc.* **58**, 515 (2011).

[10] H. Li, J. Wang, H. Liu, C. Yang, H. Xu, X. Li, H. Cui, *Vacuum* **77**, 57 (2004).

[11] E.J. Luna-Arredondo, A. Maldonado, R. Asomoza, D.R. Acosta, M.A. Meléndez-Lira, M. de la L. Olvera, *Thin Solid Films* **490**, 132 (2005).

[12] H. Abdullah, M.N. Norazia, S. Shaari, J.S. Mandeep, *Thin Solid Films* **518**, e174 (2010).

[13] M. Benhaliliba, C.E. Benouis, M.S. Aida, F. Yakuphanoglu, A.S. Juarez, *J. Sol–Gel Sci. Technol.* **55**, 335 (2010).

[14] S.B. Qadri, H. Kim, J.S. Horwitz, D.B. Chrisey, *J. Appl. Phys.* **88**, 6564 (2000).

[15] M. Girtan, G. Folcher, *Surf. Coat. Technol.* **172**, 242 (2003).

[16] S.Y. Bae, H.C. Choi, C.W. Na, J. Park, *Appl. Phys. Lett.* **86**, 033102 (2005).

[17] F. Urbach, *Phys. Rev.* **92**, 1324 (1953).